Functional and structural effects of seven-residue deletions on the coiled-coil cytoplasmic domain of a chemoreceptor

Diego A. Massazza, Silvina A. Izzo,
A. Florencia Gasperotti, M. Karina Herrera Seitz and
Claudia A. Studdert*
*Instituto de Investigaciones Biológicas, Universidad
Nacional de Mar del Plata, Mar del Plata, Buenos Aires,
Argentina.*

Summary

Chemoreceptors transmit signals from the environment to the flagellar motors via a histidine kinase that controls the phosphorylation level of the effector protein CheY. The cytoplasmic domain of chemoreceptors is strongly conserved and consists of a long alpha-helical hairpin that forms, in the dimer, a coiled-coil four-helix bundle. Changes in this domain during evolution are characterized by the presence of seven-residue insertions/deletions located symmetrically with respect to the hairpin turn, suggesting that specific interactions between the helices that form the hairpin are required for function. We assessed the impact of seven-residue deletions on the signalling ability and higher-order organization of the serine chemoreceptor from *Escherichia coli*. Our results indicate that symmetry alterations between the two branches of the cytoplasmic hairpin seriously compromise chemoreceptor function. Shorter functional versions of Tsr with symmetrical deletions form mixed trimers of dimers when coexpressed with Tar, the aspartate receptor of *E. coli*. However, Tar function in those cells is impaired, suggesting that the length difference between receptors introduces non-functional distortions into the chemoreceptor cluster. This observation is reinforced by the analysis of coexpression of Tar with chemoreceptors from *Rhodobacter sphaeroides* that naturally belong to a shorter-length class.

Introduction

Chemotactic microorganisms modulate their swimming behaviour in response to environmental stimuli, in order to seek more favourable conditions. Chemotaxis is accomplished through a signal transduction pathway that communicates intra- or extracellular signals to the flagellar motors. The system is relatively well conserved in Bacteria and Archaea (Wuichet and Zhulin, 2010), and it has been extensively studied in *Escherichia coli* (for recent reviews, see Hazelbauer *et al.*, 2008; Hazelbauer and Lai, 2010).

Chemoreceptors sense diverse stimuli and, in response, modulate the autophosphorylation activity of the histidine kinase CheA within a ternary complex that also contains the small coupling protein CheW. CheA transfers its phosphate group to the response regulator CheY. CheY-P binds to the flagellar motors and causes them to change their direction of rotation from their default counterclockwise (CCW) direction to clockwise (CW). The rapid changes in CheA kinase activity induced by stimuli are followed by a relatively slow return to the pre-stimulus activity through an adaptation process mediated by changes in the methylation level of the receptors. CheR is a dedicated methyltransferase that adds methyl groups to specific glutamyl residues, and CheB is a methylesterase that removes such methyl groups. Some of the methylatable residues are coded as glutamines and have to be converted to glutamates by CheB deamidase activity. CheB is activated by CheA-mediated phosphorylation, providing a linkage between the excitation and adaptation pathways.

Chemoreceptors, often called MCPs (for methyl-accepting chemotaxis proteins), function as homodimers. Although there are variations, most bacterial MCPs display a topology in which a ligand-binding domain is delimited by two trans-membrane segments (Lacal *et al.*, 2010). The four canonical *E. coli* MCPs belong to this topology group, and their structure is schematically represented in Fig. 1A. After the second transmembrane segment, a HAMP domain connects the periplasmic and transmembrane domains to a cytoplasmic domain consisting of a long alpha-helical hairpin that forms, in the dimer, a coiled-coil four-helix bundle (Kim *et al.*, 1999). The cytoplasmic domain is highly conserved between MCPs of different topologies and can be divided into three distinct subdomains: a strongly conserved membrane-distal protein-interaction region that mediates contacts with CheW and CheA, a membrane-proximal adaptation
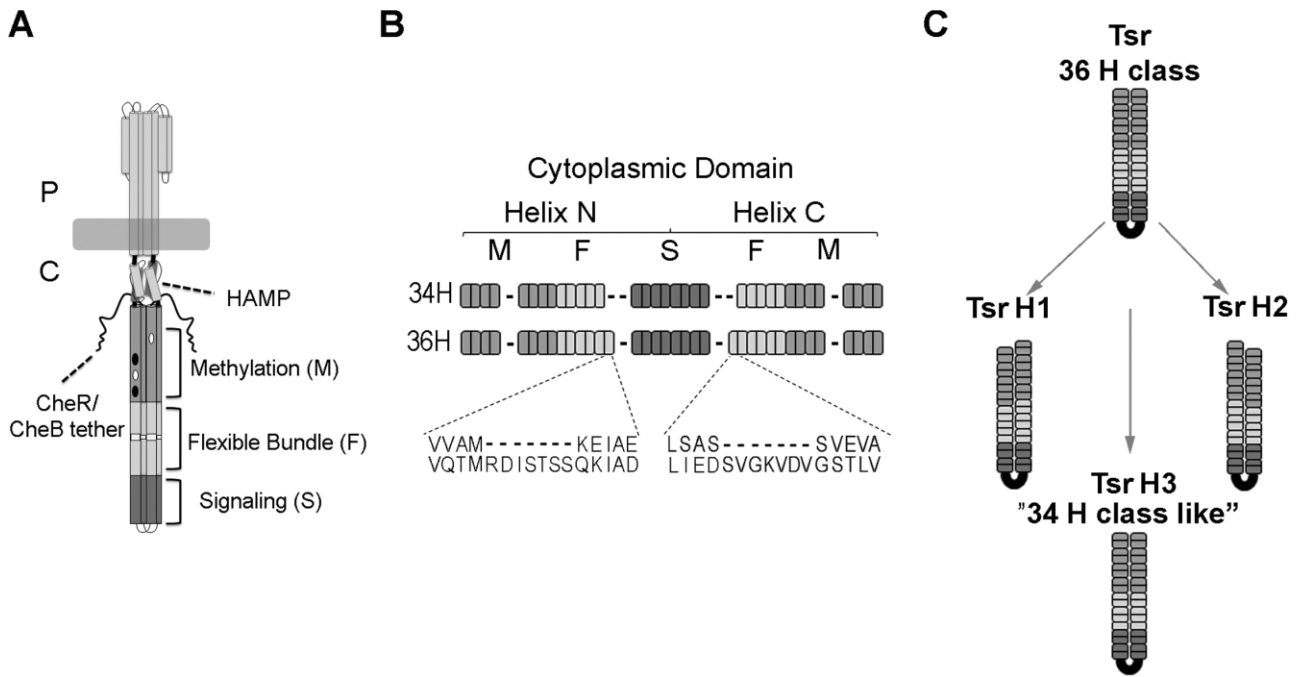
Fig. 1. Tsr-derived constructs with altered heptad content.
A. Schematic representation of a full-length dimeric Tsr receptor. The membrane is represented as a horizontal gray rectangle. The periplasmic domain of Tsr (P) is shown above the membrane plane, and the cytoplasmic domain (C) below it. Distinctive regions within the cytoplasmic domain are indicated. Oval symbols within the methylation region indicate glutaminyl (black) or glutamyl (gray) residues that are targets of the adaptation enzymes CheR and CheB. A little square in the centre of the flexible domain indicates the position of the highly conserved glycine hinge (Coleman *et al.*, 2005). The scheme is based on structural information obtained from crystals of the periplasmic domain of Tar, the aspartate receptor from *S. thyphimurium* (Yeh *et al.*, 1993), the HAMP domain of a signalling protein from *T. maritima* (Hulko *et al.*, 2006) and the cytoplasmic domain of the serine receptor Tsr from *E. coli* (Kim *et al.*, 1999).
B. Representation of the conserved cytoplasmic domain of MCPs belonging to MCP classes 36H and 34H. Each square box, divided by a vertical line, represents two heptads. Shading of the boxes follows the code of Alexander and Zhulin (2007): dashes indicate the absence of the corresponding regions as compared with the longest MCP class (44H), and shades of gray identify the characteristic regions found in the cytoplasmic domain of MCPs, as shown in A. The Tsr amino acid sequence was compared with the consensus sequence of receptors belonging to class 34H. This alignment revealed two regions of seven residues within each helix, located symmetrically with respect to the hairpin that forms the tip of the cytoplasmic domain. The corresponding sequences are shown.
C. Tsr receptor variants were constructed by deleting the corresponding heptads. The constructed variants carried a deletion in the N-helix (Tsr H1, ΔRDISTSS) in the C-helix (Tsr H2, ΔSVGKVDV), or in both helices (Tsr H3). The resulting variants are represented as forming the anti-parallel coiled-coil in which the signalling region is unaffected. The asymmetric deletions in Tsr H1 and Tsr H2 are expected to cause alterations in the interaction between N- and C-helices.

region that contains methylatable glutamyl residues, and a flexible domain that connects both regions (Alexander and Zhulin, 2007). The comparison of more than two thousand MCPs identified symmetric insertions/deletions (indels) that involve seven-residue stretches within their cytoplasmic domain (Le Moual and Koshland, 1996; Alexander and Zhulin, 2007). The indels are mainly situated in the flexible region; none of them affect the protein-interaction region. Considering the location and number of indels, as well as certain sequence features, most MCPs can be classified into one of seven major classes, named according to the total number of heptads that are present in the domain. *E. coli* MCPs belong to the 36H class, meaning that they have 18 heptads in each arm of the cytoplasmic hairpin.

The seven-residue length of the indels, corresponding to two complete alpha-helical turns, is compatible with the

preservation of the coiled-coil structure of the signalling domain. This structure would be profoundly altered by indels of different numbers of residues. Their symmetry, on the other hand, suggests the possible requirement for specific interactions between the N- and C-helices that form the long alpha-helical hairpin.

The exact mechanism by which signals generated in the ligand-binding domain or in the adaptation region are transmitted to the CheA-control region has not been completely elucidated. However, it has been demonstrated that helix–helix packing interactions within the coiled-coil are critical for this transmission (Starrett and Falke, 2005; Swain *et al.*, 2009). A recent 'yin-yang' model proposes the oppositional coupling of packing interactions between the methylation helices and the protein-interaction region (Swain *et al.*, 2009). According to this model, attractant binding causes a loosening of structural interactions in the

adaptation region that correlates with a tightening of such interactions at the cytoplasmic tip, resulting in a CheA-inhibiting conformation. Adaptation to attractants, in turn, is mediated by methylation of glutamyl residues that causes an increase in the local packing interactions. Thus, the protein-interaction region adopts a more-loosely packed conformation, and CheA activity returns to its original level. In response to repellents, the adaptation results in a decrease in methylated glutamyl residues in the methylation helices.

In this scenario, the flexible-bundle subdomain must play a key role in the transmission of conformational signals from the adaptation to the protein-interaction regions. This subdomain has a relatively low sequence conservation but always presents a group of conserved glycyl residues that constitute a 'glycine hinge'. It has been proposed that this 'hinge' is crucial for signal transmission (Coleman *et al.*, 2005).

The signalling activity of chemoreceptor dimers is somehow co-ordinated with the activity of neighbouring dimers. MCPs work together in large arrays, usually located at the poles of the cell (Maddock and Shapiro, 1993; Gestwicki *et al.*, 2000). In *E. coli*, these arrays are based in a trimer-of-dimers organization, in which MCPs of different specificities interact with each other in the protein-interaction region. This organization results in a large hexagonal array that can be imaged through cryo-electron tomography (Zhang *et al.*, 2007). The same organization has been also found in chemoreceptor arrays from microorganisms whose MCPs belong to other length classes. The correlation between measurements taken on actual chemoreceptor clusters with the predicted length of the cytoplasmic domain of the corresponding MCPs suggests that polar clusters are made up of MCPs belonging to a single class, even in organisms that code for MCPs of more than one class (Briegel *et al.*, 2009).

In this work, we assessed the impact of seven-residue deletions on the signalling abilities and higher-order organization of Tsr, the well-characterized chemoreceptor for serine in *E. coli*. Our results indicate that alterations in the symmetry of the two branches of the cytoplasmic hairpin seriously compromise chemoreceptor function. Symmetrical deletions were less disrupting, and functional serine-sensing chemoreceptors with a shorter cytoplasmic hairpin were obtained.

We also evaluated the interaction of full-length *E. coli* 36H-class receptors with the engineered 34H-class Tsr receptor and with other naturally occurring 34H-class MCPs from *Rhodobacter sphaeroides*. Our results show that MCPs from different classes can interact in mixed trimers of dimers, albeit with impaired signalling, suggesting that co-operating MCPs within a cluster must belong to the same class in order to preserve function.

Results

Construction of Tsr variants containing seven-residue deletions in the cytoplasmic domain

In order to design variants of Tsr (36H class) with alterations in the heptad content of their coiled-coil cytoplasmic domains, we compared the Tsr sequence with the consensus sequence of receptors belonging to the immediately shorter class (34H). As shown in Fig. 1B, the alignment revealed two regions of seven residues within each helix, located symmetrically with respect to the hairpin tip, which were absent in 34H-class receptors.

We introduced the corresponding deletions into Tsr by site-directed mutagenesis, obtaining three variants: Tsr H1 carries a deletion in the N-helix (residues 352–358, RDISTSS), Tsr H2 carries a deletion in the C-helix (residues 424–430, SVGKVDV), and Tsr H3 bears both deletions, located symmetrically, thus mimicking a chemoreceptor that belongs to the 34H class. Figure 1C shows schematic representations of the three variants. In these representations, we assumed that the folding at the cytoplasmic hairpin was unaffected.

For simplicity, we refer to specific residues in the Tsr-derived constructions using Tsr numbering, irrespective of the presence of deletions. If the numbering in a specific construct does not correspond to the wild-type Tsr numbering, the number is shown in italics.

In order to assess the stability of the resulting proteins, the three Tsr variants were expressed at physiological levels in a strain lacking all other chemotaxis proteins, and the Tsr content was compared to that of wild-type Tsr by immunoblotting (Fig. 2A). All three Tsr derivatives were expressed at a level comparable to wild-type Tsr, indicating that the introduced deletions did not significantly affect protein stability. The three Tsr-derived proteins displayed very similar electrophoretic mobilities, irrespective of the presence of one, the other, or both deletions.

Functional characterization of the heptad-deletion Tsr variants

Semi-solid agar plates. The ability of the Tsr variants when present as the only receptor in the cell to mediate chemotaxis to serine was analysed in semi-solid agar plates (Fig. 2B). None of the Tsr derivatives was able to complement Tsr function. Cells expressing the double-deletion construct Tsr H3 formed larger colonies than those harbouring Tsr H1 or Tsr H2. However, this behaviour did not represent true chemotaxis toward serine, because it did not result in the sharp, continuously expanding ring formed by cells expressing wild-type Tsr. The absence of complementation was observed over a broad range of inducing conditions for all three variants (data not shown).
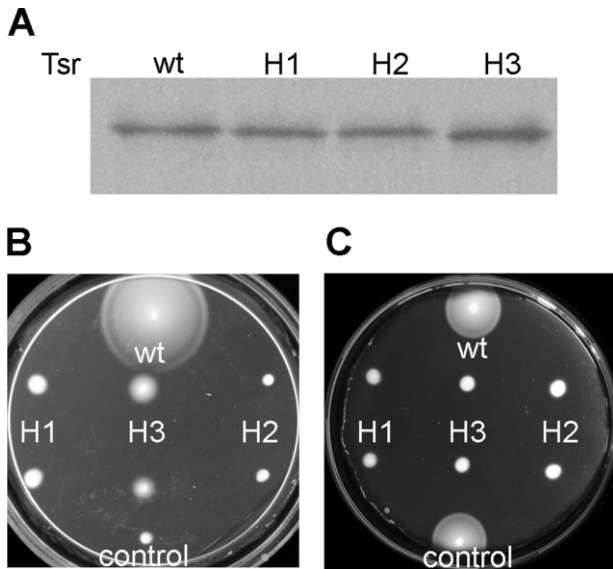
A

Tsr   wt   H1   H2   H3

B   C

Fig. 2. Expression and functional analysis of the Tsr-variant constructs.
A. Expression of Tsr-derivatives. UU1581 cells (ΔMCPs, Δche), cells carrying pCS12 (Tsr) or derivatives (H1, H2, H3) were grown to mid-log phase in the presence of 0.45 μM sodium salicylate. Cells were harvested by centrifugation and lysed in sample buffer. Proteins from the lysed cells was analysed by SDS-PAGE in a 12% acrylamide, 0.32% bisacrylamide gel and visualized by immunoblotting using an anti-Tsr antibody.
B. Tsr function in the absence of other receptors. UU1250 cells (lacking MCPs) carrying the empty vector plasmid pKG116 (control), pCS12 (wild-type Tsr, wt) or two colonies of each Tsr derivative (H1, H2, H3) were inoculated into semi-solid T-agar plates containing 12.5 μg ml^{-1} chloramphenicol and 0.45 μM sodium salicylate and incubated for 8 h at 30°C.
C. Tar function in the presence of Tsr derivatives. UU1624 cells (lacking all MCPs except Tar) carrying the empty vector plasmid pKG116 (control), pCS12 (wild-type Tsr, wt) or two colonies of each Tsr derivative (H1, H2, H3) were inoculated into minimal aspartate semi-solid agar plates containing 12.5 μg ml^{-1} chloramphenicol and 0.45 μM sodium salicylate and incubated for 20 h at 30°C.

The effect of the Tsr variants on chemotaxis mediated by a full-length receptor of a different specificity was also analysed. The Tsr-deletion constructs were expressed in a strain that also expresses Tar, the aspartate receptor, as its only chemoreceptor. In order to assess Tar function only, assays were performed in minimal-aspartate semi-solid agar plates. Although the expression of wild-type Tsr had no effect on the size or appearance of the aspartate ring, all three deletion constructs strongly interfered with aspartate chemotaxis, even at moderate levels of induction (Fig. 2C).

With the aim of understanding why the Tsr-deletion constructs failed to complement Tsr function, different signalling abilities were analysed in cells expressing the three variants. We investigated their ability to activate the kinase CheA, their ability to modulate CheA activity in response to an attractant, and their ability to respond to addition of an attractant with an increase in methylation level.

Kinase control in tethered cells. CheA control was first assessed through the analysis of the rotational behaviour of cells tethered to a coverslip by a single flagellum. Cells devoid of chemoreceptors have extremely low levels of phosphorylated CheY, which can only be produced through basal CheA activity. As a consequence, their flagella rotate almost exclusively in the default CCW direction. CheA activation, induced by expression of any MCP that is able to form active ternary complexes with CheA and CheW, results in an increase in the level of CheY-phosphate, which in turn causes episodes of CW rotation. Also, the ability to modulate CheA kinase activity is easily observed in this assay, because the addition of attractant causes an immediate inhibition of CW rotation in cells expressing fully functional receptors.

In UU1250 cells, which lack all five native chemoreceptors but are otherwise proficient for chemotaxis, we were able to compare the level of CheA activation reached by the Tsr-derived constructs with that mediated by wild-type Tsr. As can be seen in Fig. 3 (top left panel), flagella from cells expressing wild-type Tsr spent 38% of their time in CW rotation, and this value dropped to zero upon addition of serine concentrations as low as 10 μM. Tsr H2, which bears the heptad deletion in the C-helix, was absolutely unable to activate the kinase (Fig. 3, bottom left panel), but both Tsr H1 and Tsr H3 activated CheA to high levels (74.5 and 72% CW rotation in the absence of serine respectively; Fig. 3, right panels). The two CheA-activating variants showed differences in their ability to inhibit CheA in response to attractants. Tsr H1 was completely insensitive to the addition of serine concentrations as high as 100 mM (Fig. 3, top right panel). In contrast, the double-deleted Tsr H3 inhibited CheA upon addition of 10 mM serine (0.05% CW) and even showed a weak response to 10 μM serine (52% CW), indicating that it was responsive to serine, but with much lower sensitivity than wild-type Tsr (Fig. 3, bottom right panels).

When the same experiments were carried out using the UU1535 strain, which lacks all five native chemoreceptors as well as the adaptation enzymes CheR and CheB, wild-type Tsr behaved as expected (70% CW rotation in the absence, and no CW rotation in the presence, of 10 mM serine, Fig. S1A). However, although both Tsr H1 and Tsr H3 activated the kinase as in UU1250 cells, the ability of Tsr H3 to respond to serine was lost, even at an extremely high serine concentration (up to 500 mM), indicating that, in the absence of CheB-mediated deamidation of glutaminyl residues in the adaptation region, this variant displays a locked-on conformation (Fig. S1A).

Because Tsr H2 did not activate the kinase in any of the two strains mentioned above, its ability to control CheA was assayed in the presence of other CheA-activating receptors. We used a strain, MDP1, which lacks only Tsr and is extremely CW-biased due to the absence of the
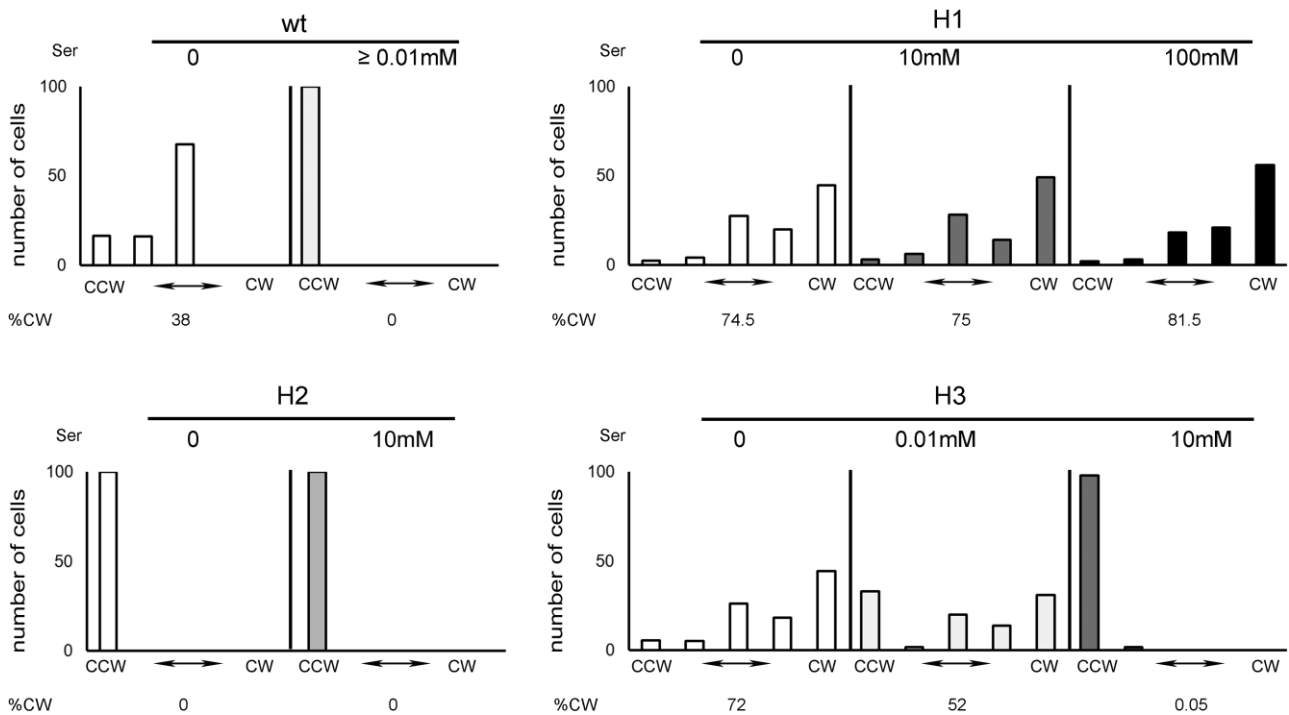
Fig. 3. Receptor-mediated control of CheA kinase. The rotational behaviour of UU1250 cells (ΔMCPs) expressing wild-type Tsr or its derivatives was analysed in a tethering assay. Cells were observed in the absence of stimulus or in the presence of the indicated concentrations of L-serine. One hundred cells were observed for each treatment over 15 s and classified into one of five categories, ranging from exclusively CCW to exclusively CW. The time that cells spent in CW rotation was calculated as described in *Experimental procedures* and is indicated below each graph. In all cases, cells were observed within less than 3 min after the addition of attractant.

phosphatase CheZ. In this strain, wild-type Tsr was able to inhibit CheA in response to serine, whereas Tsr H2 was completely insensitive to it (Fig. S1B). Tsr H1 was again completely insensitive, and Tsr H3 displayed only a partial response to 10 mM serine, showing once again that the double-deletion variant is able to respond to serine, but with much-reduced sensitivity (Fig. S1B).

Taken together, the CheA-control experiments allow us to conclude that the seven-residue deletion in the N-helix generates a receptor that is still able to activate CheA but is insensitive to attractants. The deletion in the C-helix disrupts both CheA-activating and CheA-modulating abilities of the receptor, and the variant bearing symmetrical deletions in both helices activates the kinase and displays a partial response to serine when CheR and CheB are present in the cell.

Serine response in free-swimming cells. The partial ability of Tsr H3 to inhibit CheA in response to serine can be studied in the CheZ phosphatase-lacking strain MDP1. This strain tumbles continuously because of the high levels of CheY-phosphate generated by CheA in the presence of all the native receptors except Tsr. MDP1 cells expressing wild-type Tsr responded to the addition of 100 μM serine with immediate smooth-swimming behaviour that slowly reverted to the original tumbly behaviour.

Cells retained a significant level of smooth swimming 6 min after the addition of attractant (*Supporting information*, MDP1-Tsr.mpg). In contrast, cells expressing Tsr H3 displayed a very weak and transient smooth-swimming response to the same serine concentration; cells swam rather wobbly and with shorter runs. Moreover, 3 min after the addition of serine, they were as tumbly as before its addition (*Supporting information*, MDP1-Tsr H3.mpg).

Methylation response. In order to assess the ability of the Tsr variants to respond to attractants by undergoing CheR-mediated adaptation, we next analysed their methylation patterns. The methylation level of the receptor variants was inferred by their electrophoretic behaviour (Draheim *et al.*, 2005), both in the unstimulated baseline condition and after exposure to a high concentration of serine. In order to avoid any influence of the differences in the CheA-activation ability of the constructs that would result in differences in CheB methylesterase activity, we used UU1626 cells, which lack all five native receptors as well as CheA and CheW. In these cells, the methylation pattern should be independent of CheB phosphorylation and depend only on the conformation of the receptors in the absence or presence of attractant.

As shown in Fig. 4, wild-type Tsr showed a marked increase in electrophoretic mobility when cells were
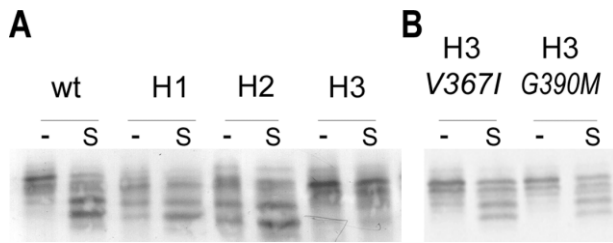
A

Fig. 4. Methylation response to attractant addition.
A. UU1626 cells (ΔMCPs, ΔcheA, ΔcheW) carrying pCS12 (wild-type Tsr, wt), or Tsr derivatives (H1, H2, H3), were grown to mid-log phase in the presence of 0.45 μM sodium salicylate. Cells were harvested by centrifugation, washed twice, and resuspended in methylation buffer. After 15 min at 30°C, cells were challenged with water (-) or 100 mM L-serine (S) for 30 min. Cells were harvested and boiled in sample buffer. Proteins from the lysed cells were analysed in low bisacrylamide SDS-PAGE gels and visualized by immunoblotting using an anti-Tsr antiserum. Faster-migrating bands represent more-highly methylated species.
B. The same experiment was carried out with UU1626 cells expressing the pseudo-revertants Tsr H3 *V367I* or Tsr H3 *G390M*.

exposed to serine, indicating an increase in its methylation level. The asymmetric variants Tsr H1 and Tsr H2 showed a significantly higher basal methylation level and, when stimulated with serine, showed a slight increase in their methylation levels. On the other hand, Tsr H3 showed a wild-type pattern of basal methylation, but exhibited only very small changes in mobility upon exposure to attractant, suggesting that the conformational change caused by serine binding was rather subtle and/or very transient, as it presumably was in the H1 and H2 variants.

Higher-order organization and polar clustering

In vivo *cross-linking assays.* In previous studies, we used the tri-functional cross-linker tris-(2-maleimidoethyl)-amine (TMEA) and cysteine-substituted transducers to show that receptors of the same or different specificity are arranged in trimers of dimers *in vivo* (Studdert and Parkinson, 2004; Massazza *et al.*, 2011). The observed cross-linking was consistent with an arrangement in which the contacts between dimers at the cytoplasmic tip are similar to the ones observed in the crystal structure of the cytoplasmic domain of Tsr (Kim *et al.*, 1999).

To analyse the *in vivo* organization of the heptad-deleted constructs, we first analysed whether their over-expression interferes with the formation of two- and three-subunit cross-linking products in cells expressing chromosomal levels of Tar S364C, which bears the cysteine cross-linking reporter (competition assay, Studdert and Parkinson, 2005). This assay allows the distinction between receptors that are proficient in trimer formation (competitors) and those that are not (non-competitors). Competitors incorporate into mixed trimers of dimers and significantly decrease the abundance of Tar-only trimers. Non-competitors are unable to get incorporated into

mixed trimers with Tar. We observed that the symmetric variant Tsr H3 clearly decreased the amount of Tar S364C cross-linking products when it was overexpressed, indicating that it could interact with full-length Tar in trimers of dimers. Tsr H2 behaved as a total non-competitor, even at very high levels of expression. Overexpression of Tsr H1 partially decreased the amount of Tar S364C three-subunit cross-linked products, suggesting that Tsr H1 retains some ability to interact with full-length Tar in mixed trimers of dimers (Fig. S2).

In order to characterize the trimer-forming ability of the variants in more detail, the equivalent cysteine reporter in Tsr, S366C, was introduced into each construct. The ability of the cysteine-substituted variants to form two- and three-subunit products was assessed by TMEA-mediated cross-linking in cells in which the receptors were expressed at physiological levels of induction.

We first assessed the formation of cross-linking products after TMEA treatment in UU1581 cells, in the absence of other receptors and chemotaxis proteins (Fig. 5A). The symmetric construct Tsr H3 showed a wild-type ability to form cross-linking products (Fig. 5A, compare first and last lanes), whereas cross-linking products were barely detectable from either construct bearing an asymmetric deletion (Fig. 5A, middle lanes). To study the ability of the variants to form mixed trimers with full-length Tar, the same experiment was conducted in cells expressing Tar S364C. Mixed products between Tar S364C and Tsr H3 *S366C* were clearly observed (Fig. 5B). In contrast, no mixed products were observed between Tar S364C and Tsr H1 or H2 bearing the *S366C* reporter (Fig. 5B).

The cross-linking pattern of Tsr H3 was consistent with its behaviour in the competition assay; this construct is able to form trimers by itself and to form mixed trimers with full-length Tar, with cross-linking patterns similar to those displayed by wild-type Tsr. The results obtained with Tsr H2 are consistent with the inability of this construct to form trimers by itself or with Tar. The results obtained with Tsr H1, however, seem contradictory. On the one hand, in competition assays this construct could interfere with the formation of Tar cross-linking products to some degree, suggesting that it retains certain ability to form mixed trimers. Nevertheless, Tsr H1 *S366C* did not generate any significant amount of cross-linking products, either by itself or with full-length Tar S364C. One possibility is that Tsr H1 incorporates into mixed trimers with Tar to a certain extent, but that a conformational distortion alters the geometry of the reporter, thus rendering it incapable of forming cross-linked trimers with the rigid and planar tri-functional reagent TMEA.

Polar localization.

Polar localization. In wild-type cells, chemoreceptors are localized in tight, polar clusters together with the coupling protein CheW, the kinase CheA, the adaptation enzymes
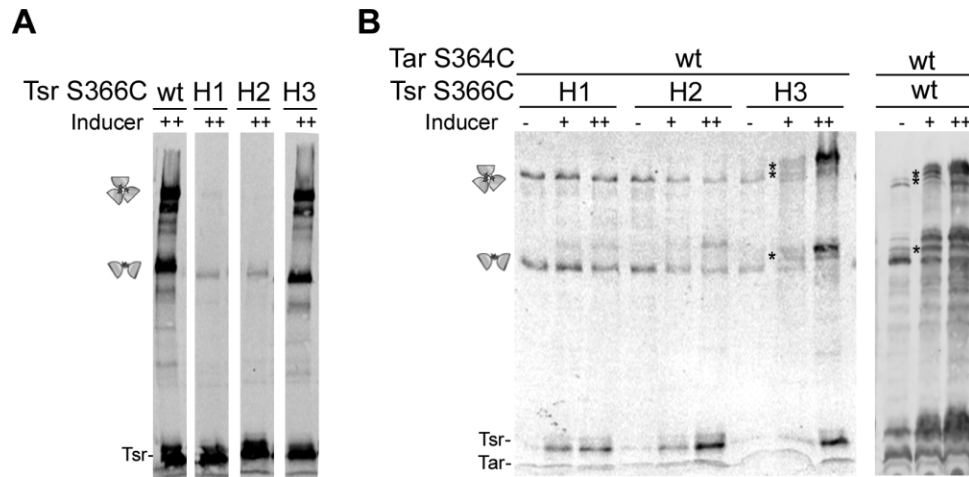
A

B

Fig. 5. *In vivo* cross-linking assays. Strains expressing single cysteine-substituted Tsr receptor or cysteine-substituted Tsr variants were grown to mid-log phase, treated with the cross-linker TMEA, analysed by SDS-PAGE gels, and visualized by immunoblotting with an anti-Tsr antibody that reacts with both Tsr and Tar. Tsr expression was induced at 0 (-), 0.15 (+) or 0.30 (++) µM sodium salicylate. Cartoons on the left indicate the region of the gel where two- and three-subunit cross-linking products were found.
A. UU1581 cells (lacking any other chemotaxis protein) carrying pCS12 S366C (wild-type Tsr, wt) or its cysteine-substituted derivatives (H1, H2, H3).
B. UU1613 cells (carrying a chromosomal copy of Tar S364C expressed from its native promoter and lacking CheAWRB and other MCPs) transformed with plasmid pCS12 S366C (wild-type Tsr, wt) or its cysteine-substituted derivatives (H1, H2, H3). Mixed cross-linking products are denoted with asterisks.

CheR and CheB, and the phosphatase CheZ (Sourjik and Berg, 2000). The CheR methyltransferase binds to a C-terminal pentapeptide that is present in the two major chemoreceptors, Tsr and Tar. A YFP–CheR fusion protein was used to analyse the subcellular localization of the Tsr-derived constructs by fluorescence microscopy, using a strain lacking MCPs, CheR and CheB (UU1535). The CheA-activating constructs Tsr H1 and Tsr H3 localized YFP–CheR to the poles with an efficiency comparable to that of wild-type Tsr (more than 70% of cells with polar clusters, Fig. 6). In contrast, Tsr H2 receptors showed a significantly reduced ability to localize YFP–CheR to the poles (about 30% of cells with polar clusters, Fig. 6). These results are consistent with the ability of the Tsr H1 and Tsr H3 constructs to form trimers of dimers and to activate the kinase, whereas Tsr H2 is incapable of either function.

Tsr H3 derivatives with restored ability to mediate serine chemotaxis

In order to assess the severity of the alterations carried by the three Tsr-derived constructs, we decided to look for mutations at a second site that could correct their functional defects.

Plasmids encoding the different variants were randomly mutagenized and introduced into UU1250 cells, which lack all five native receptors. Transformant pools were streaked in semi-solid tryptone agar plates in order to isolate functional derivatives, which were identified by the outgrowth of chemotactic rings from the streaks.

Similar numbers (about 10[7]) of independent transformants were analysed from each pool of mutagenized plasmids. No functional derivatives were found with the constructs bearing single heptad deletions. In contrast,
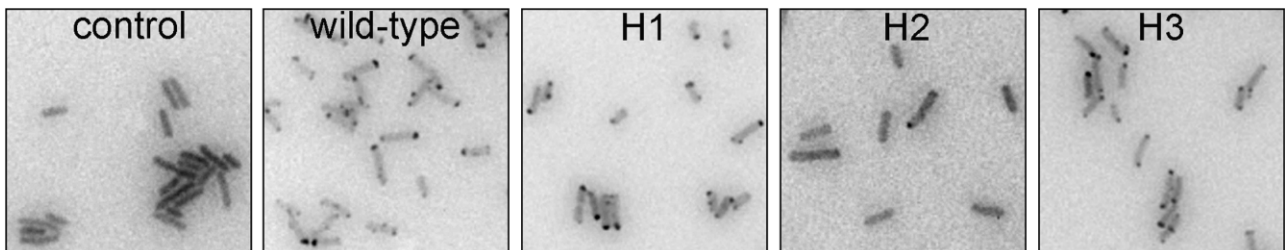

Fig. 6. Polar localization. UU1535 cells (ΔMCPs, ΔCheRB) carrying plasmid pPA803 (YFP–CheR under IPTG control) and plasmid pKG116 (control), pCS12 (wild-type Tsr), or its cysteine-substituted derivatives (H1, H2, H3), were grown at 30°C in tryptone broth to mid-log phase in the presence of 100 µM IPTG and 0.45 µM sodium salicylate. Cells were then examined by fluorescence microscopy.
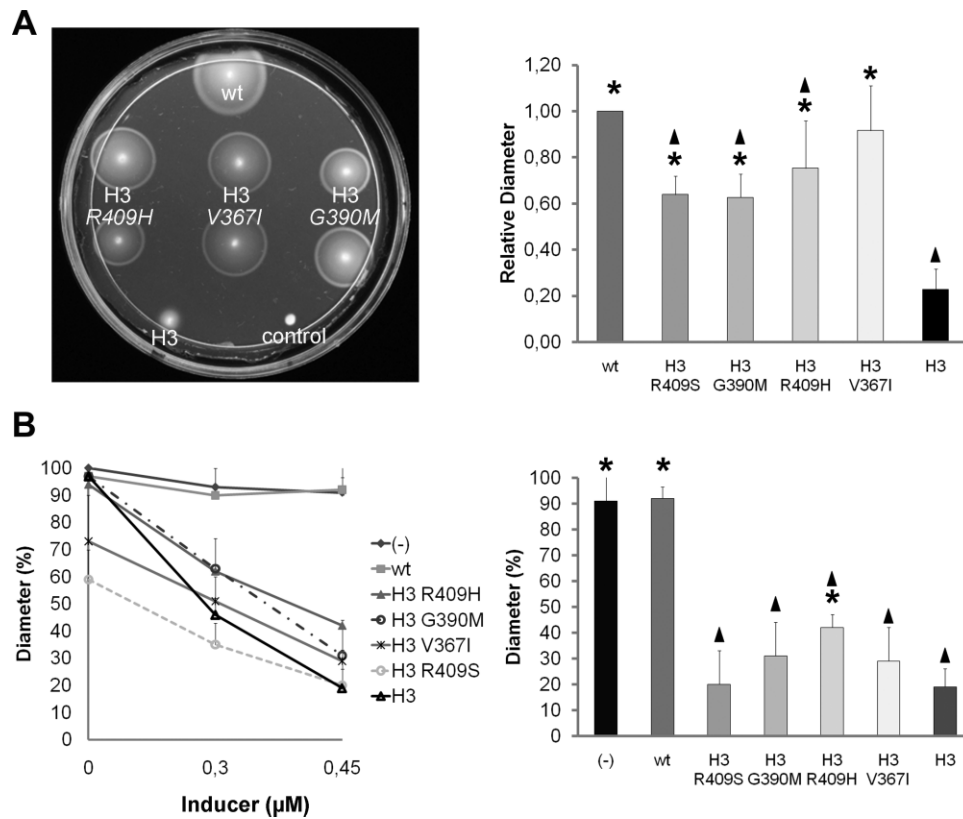
Fig. 7. Functional analysis of pseudo-revertants in semi-solid agar plates. Functional derivatives of Tsr H3 (Tsr H3* variants) isolated as described in the text were analysed in semi-solid agar plates for Tsr function and their effect on Tar function.
A. UU1250 cells (ΔMCP) carrying the empty vector plasmid pKG116 (control), plasmid pCS12 (wild-type Tsr, wt), plasmid pTsr H3 derivative (H3) or two colonies of each of the indicated H3-derived point mutants were inoculated in tryptone semi-solid agar plates containing 12.5 μg ml⁻¹ chloramphenicol and 0.45 μM sodium salicylate and then incubated for 8 h. On the left, a representative semi-solid agar plate is shown. The histogram on the right shows the ring diameter of cells bearing the H3 receptor or its pseudo-revertant relative to the ring diameter of wild-type Tsr. Significant differences ($P < 0.05$) with respect to wild-type Tsr are indicated with ▲. Significant differences ($P < 0.05$) with respect to the parental H3 receptor are indicated with *. The data are presented as means and standard deviations of the mean based on three images taken from independent experiments.
B. UU1624 cells (lacking all MCPs except Tar) carrying the empty vector plasmid pKG116 (control), plasmid pCS12 (wild-type Tsr, wt), the Tsr H3 derivative (H3) or the indicated H3-derived point mutants were inoculated in minimal-aspartate semi-solid agar plates containing 12.5 μg ml⁻¹ chloramphenicol and different concentrations of sodium salicylate and incubated for 20 h. The left panel shows the diameter of the resulting aspartate rings normalized to the average diameter displayed by the colonies of cells containing the empty vector with no induction. On the right, the same information is shown after induction with 0.45 μM sodium salicylate. Significant differences ($P < 0.05$) with respect to the wild-type Tsr receptor are indicated with ▲. Significant differences ($P < 0.05$) with respect to the parental H3 receptor are indicated with *. The data are presented as means and standard deviations of the mean based on three images taken from independent experiments.

mutagenized plasmids encoding Tsr H3 gave rise to derivatives that were able to form serine rings in semi-solid agar plates (Fig. 7A, left). Even though the rings were, in some cases, qualitatively different from those generated by wild-type Tsr, they did represent true chemotaxis towards serine, as the rings were sharp and expanded continuously. After 8 h incubation, their diameters were significantly larger than the diameter of the parental Tsr H3 colony (Fig. 7A, right panel and Fig. S3). The subsequent sequence analysis of these Tsr H3 pseudo-revertants (which we collectively named Tsr H3*) identified the single-residue substitutions that were responsible for regaining serine-sensing abilities (G390M,

R409S, R409H and V367I). Notably, all four substitutions were located in the signalling domain. When introduced into full-length Tsr, these substitutions impaired chemotaxis to serine to some extent, with R409H being the most severely affected (Fig. S3).

The Tsr H3* constructs behaved much as wild-type Tsr, both with respect to their methylation responses (see examples in Fig. 4B) and with respect to their sensitivities to serine for inhibiting kinase activity (*Supporting information*, MDP1-Tsr H3 V367I.mpg). However, they were all strongly epistatic when coexpressed with full-length Tar, clearly interfering with the development of chemotactic rings in minimal-aspartate semi-solid agar plates at physi-
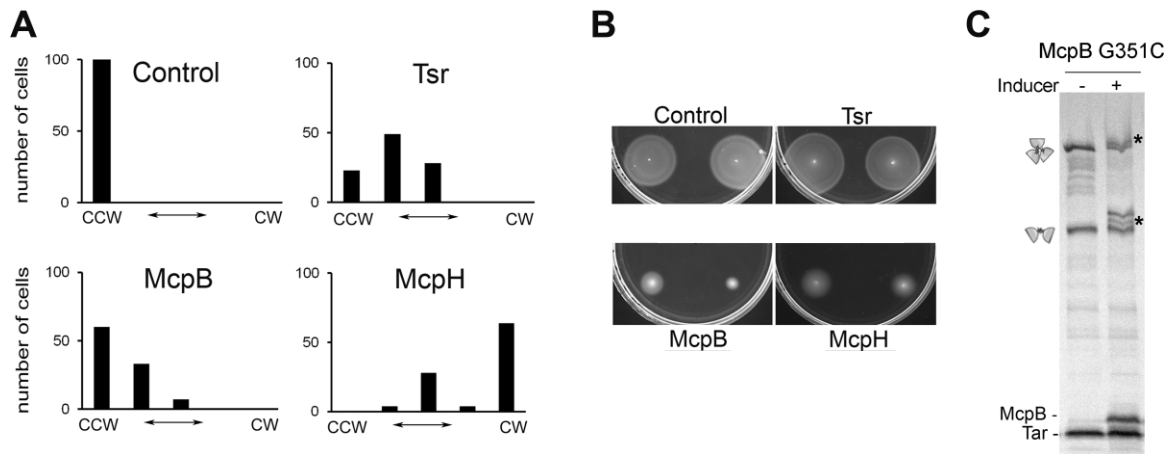
Fig. 8. Expression of McpB or McpH from *Rhodobacter sphaeroides* 2.4.1 in *E. coli*.
A. Rotational behaviour of UU1250 cells (ΔMCPs) expressing no MCP (control) or the indicated receptors. MCP expression was induced at 0.45 μM sodium salicylate. Cells were observed in the presence of tethering buffer. One hundred cells were observed for 15 s each and classified into one of five categories, from exclusively CCW to exclusively CW.
B. Tar function in the presence of 34H-class receptors. UU1624 cells (lacking all MCPs except Tar) carrying the empty vector plasmid pKG116 (control), plasmid pCS12 (wild-type Tsr), pFG2 (McpB) or pK5 (McpH) were inoculated into minimal-aspartate semi-solid agar plates containing 12.5 μg ml⁻¹ chloramphenicol and 0.45 μM sodium salicylate and then incubated for 20 h at 30°C.
C. *In vivo* cross-linking assay. UU1613 cells (carrying a chromosomal copy of Tar S364C expressed from its native promoter and lacking CheAWRB and other MCPs) transformed with pFG2 G351C (McpB G351C) were grown to mid-log phase with 0 (-) or 0.7 μM sodium salicylate (+), treated with the cross-linker TMEA, analysed by SDS-PAGE, and visualized by immunoblotting with an anti-Tsr antibody, which reacts with both McpB and Tar. Mixed cross-linking products are denoted with asterisks.

ological levels of induction (Fig. 7B, right panel). The interference was as strong as that displayed by the Tsr H3 parental construct, in spite of the fact that the mutagenized variants now functioned as competent serine-sensing receptors. As can be seen in the graph (Fig. 7B, left panel), some of the Tsr H3* variants interfered with Tar function even at very low levels of expression, suggesting that their effect is due to some distorting interaction within the chemoreceptor cluster, rather than to titration of other components.

We then analysed the influence of Tar expression on serine taxis mediated by one of the Tsr H3* functional variants. To that end, we introduced the coding region of Tsr H3 V367I into the chromosome, at the normal *tsr* locus, in cells that lacked any other MCP. Then, chemotaxis towards both serine and aspartate was evaluated in semi-solid agar tryptone plates as Tar was expressed from a salicylate-inducible plasmid. Quite surprisingly, the formation of the aspartate ring did not correlate with any alteration of the serine ring mediated by the Tsr H3* receptor (Fig. S4). This result suggests that the formation of mixed trimers between chemoreceptors of different lengths has a negative impact on the function of the longer receptor, whereas the function of the shorter one remains unaffected. We speculate that Tsr H3 V367I can function both in pure trimers and mixed trimers with full-length Tar. In contrast, Tar displays defective function when it is forced to be part of mixed trimers with the shorter receptor. However, when

the relative expression level of Tar ensures the formation of a sufficient amount of pure Tar trimers, the deleterious effect of Tsr H3 V367I on Tar function is overcome.

Coexpression of natural 34H class receptors with Tar

In order to investigate whether natural receptors belonging to the 34H class can interact with 36H-class receptors in mixed trimers, we expressed McpB or McpH from *R. sphaeroides* 2.4.1 (belonging to class 34H) in *E. coli* cells and evaluated their ability to activate the kinase and to form mixed trimers of dimers with Tar.

Both 34H-class receptors were able to activate the CheA kinase when expressed as the only MCP in UU1250 cells (Fig. 8A). Also, both receptors showed partial competition in TMEA-cross-linking assays, indicating that they were incorporated into mixed trimers with Tar S364C, and then significantly decreased the amount of three-subunit Tar S364C products (Fig. S2). To confirm that the competition was due to the ability of these receptors to form mixed trimers, we introduced a cysteine residue into McpB at position 351 (equivalent to S364 in Tar). TMEA-cross-linking assays were performed with cells coexpressing Tar S364C from the chromosome and McpB G351C from a plasmid. McpB G351C was clearly able to form cross-linked products with Tar S364C upon TMEA treatment, indicating that it was incorporated into mixed trimers of dimers (Fig. 8C).
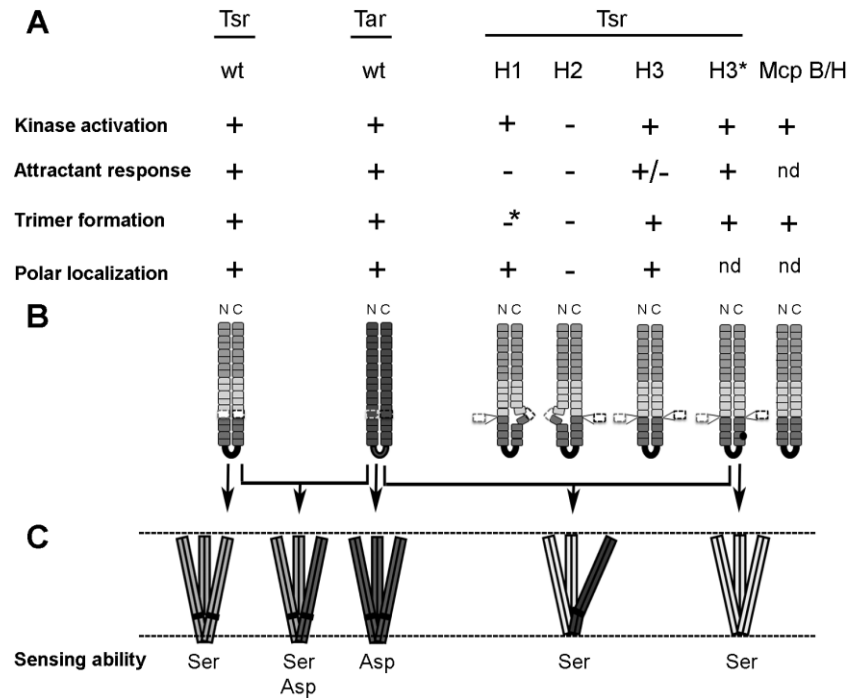
	Tsr	Tar	Tsr				
	wt	wt	H1	H2	H3	H3*	Mcp B/H
Kinase activation	+	+	+	-	+	+	+
Attractant response	+	+	-	-	+/-	+	nd
Trimer formation	+	+	-*	-	+	+	+
Polar localization	+	+	+	-	+	nd	nd

Fig. 9. Effect of heptad deletions on Tsr function.
A. Summary of the most relevant results. Plus and minus signs indicate the presence or absence of the indicated features displayed by the different MCP variants; nd indicates not determined. The asterisk on the minus sign for Tsr H1 trimer formation denotes that the experiments gave somewhat conflicting results, as discussed in the text.
B. Schematic representation of monomers corresponding to each MCP or MCP variant. Boxes divided by a central line represent two heptads, and their shading corresponds to the different subdomains as in Fig. 1. The heptads that were targets for deletion are represented as half-boxes with dashed borders. Deleted heptads are drawn to the side. In this scheme, most of the normal interactions between the N- and C-helices are unaffected. We postulate that the asymmetrically deleted constructs contain a distortion in the longer helix in the region corresponding to the unpaired heptad and those in its immediate vicinity. The small dot on Tsr H3* represents any of the four replacements that render this construct proficient for serine-sensing.
C. Schematic representation of trimers formed by different combinations of MCPs or MCP variants. Each dimer is represented by a rectangle that is divided vertically to indicate two receptor homodimers. On the left side, trimers made of 36H-class dimers are shown: from left to right, a pure Tsr trimer (medium gray), a mixed Tsr-Tar trimer and a pure Tar trimer (dark gray). In each 36H dimer the region that was deleted to make the 34H-class derivative is shown in black. On the right, shortened serine-sensing Tsr H3* dimers (light gray) forming a pure trimer and a mixed trimer (containing two 34H-class Tsr H3* dimers and a 36H-class Tar dimer) are shown to indicate that a distortion caused by the difference between full-length Tar and Tsr H3* might impair Tar function in the mixed trimer. The dashed lines indicate the distance between the membrane-proximal portion of the domain and the distal cytoplasmic tip.

Finally, the effect of McpB or McpH expression on Tar function in semi-solid agar plates was evaluated. As had been observed with the 34H-class Tsr H3* variants, the expression of McpB or McpH strongly interfered with Tar function, even at moderate levels of induction (Fig. 8B). These results suggest that the functional interference may derive from a distortion of Tar-containing trimers that incorporate receptors of the 34H class. This distortion would presumably have a negative impact on cluster organization and/or receptor signalling.

Discussion

We sought to understand the functional requirements of the coiled-coil four-helix bundle present in the cytoplasmic domain of MCPs, a structure that has undergone a peculiar evolutionary history. To that end, we engineered derivatives of the 36-heptad-repeat (36H class) receptor Tsr to mimic receptors in the immediately shorter 34H class. Seven-residue deletions introduced into the N-terminal, the C-terminal, and both arms of the cytoplasmic domain of Tsr produced non-functional derivatives. However, each of the three alterations led to remarkably different receptor behaviours, which are summarized in Fig. 9.

Asymmetric heptad deletions (Tsr H1 and Tsr H2)

A heptad deletion in only one helix of the hairpin could, in principle, affect the folding of the coiled-coil cytoplasmic domain in different ways. One possible folding would be driven by interactions between heptads in the kinase-control domain that are close to the hairpin turn, as schematically depicted in Fig. 1C. If this were the case, then

we would expect that both asymmetrically deleted constructs would display activities comparable to those of wild-type Tsr in stimulating the CheA kinase, as this ability resides in the region that surrounds the hairpin turn (Ames and Parkinson, 1994). However, our results show that Tsr H2, which carries a heptad deletion in the C-helix, is absolutely unable to activate the kinase, whereas Tsr H1, with a heptad deletion in the N-helix, activates CheA even more efficiently than wild-type Tsr. It could be argued that Tsr H2 has undergone dramatic alterations in its structure because, in addition to its inability to activate CheA, it is unable to mediate any response to serine even in the presence of other receptors (Fig. 3). It also fails to form trimers of dimers (Fig. 5) or to localize efficiently to the poles of the cell (Fig. 6). However, its stability and its ability to interfere with Tar function at physiological levels of expression (Fig. 2C) argue in favour of its assuming a conformation that still allows interactions with other receptors or signalling proteins.

The second possibility is that strong interactions between heptads far away from the tip, in the adaptation region, for example, create a situation in which the longer helix develops some kind of bulge between that region and the hairpin turn, as is schematically depicted in Fig. 9B. Most of the native interactions between the N- and C-helices would be preserved, with the alterations largely restricted to the vicinity of the unpaired heptad in the longer helix, which would bulge out as a loop. The shorter helix, bearing the deletion, would be less altered. We speculate that this might be why the Tsr H1 construct has some ability to form trimers of dimers (Fig. S2), because most of the residues involved in dimer-to-dimer contact within the trimer are located in the N-helix (Kim *et al.*, 1999). Tsr H1 also shows wild-type ability to localize to the poles of the cell (Fig. 6). However, it cannot inhibit CheA in response to serine (Fig. 3), and it shows a very small increase in methylation in response to addition of serine (Fig. 4).

The introduction of a single-heptad deletion in the N- or in the C-helix would be expected to alter the structural elements called 'knobs' and 'sockets', which are characteristic of coiled-coils. A protuberant 'knob' residue fits into a 'socket' made by four residues in a neighbouring helix (Walshaw and Woolfson, 2003). It has been previously shown that the weakening of any of several conserved knob-and-socket pairs in Tar by replacement of the bulky knob residue by a small alaninyl residue significantly perturbs receptor function (Swain *et al.*, 2009). The essential knob-and-socket interactions required for proper receptor function are located in the adaptation and protein-interaction regions (Swain *et al.*, 2009). Even though the heptad deletions in this study were introduced into the flexible region, in which no conserved knob-and-socket pairs have been identified, the proposed folding could

presumably alter the pairing of the heptads that lie immediately after (for Tsr H1) or immediately before (for Tsr H2) the bulge, which belong to the protein-interaction region (see schemes in Fig. 9). It is not surprising, then, that both Tsr H1 and Tsr H2 are dysfunctional. A characteristic shared by both asymmetric constructions was their substantially elevated baseline level of covalent modification. This property could be explained by an increased accessibility to the CheR methyltransferase, which might derive from the inability to form trimers of dimers (for Tsr H2) or the formation of distorted trimers of dimers (for Tsr H1). It has been previously shown that disruptions of the trimer structure correlate with elevated methylation levels (Cardozo *et al.*, 2010). Alternatively, the elevated covalent modification might represent the inability of one or both constructs to serve as substrates of the CheB methylesterase/deaminase.

Symmetric heptad deletions in both helices (Tsr H3)

In contrast with Tsr H1 and Tsr H2, the construct bearing matching deletions in both the N-terminal and C-terminal helices showed wild-type ability to form trimers of dimers in competition assays (Fig. S2) and by direct cross-linking with the tri-functional reagent TMEA (Fig. 5A). This construct displays a partial lock-on character, suggesting that the structure of the flexible bundle subdomain plays an important role in the balance between the 'on' and 'off' conformations of the receptors, as well as in the proper transmission of the signals sensed by the ligand-binding domain. Comparable matching deletions encompassing two heptads in each helix of the flexible bundle domain of DifA, an MCP-like sensory transducer from *Myxococcus xanthus*, has also been correlated with a constitutively active conformation (Xu *et al.*, 2011). Even though Tsr H3 did not complement Tsr function in semi-solid agar plates (Fig. 2B), it displayed a partial ability to mediate a serine response in tethered and in free-swimming cells, indicating that it retains some ability to inhibit CheA activity in response to attractants (Fig. 3 and *Supporting information*, MDP1-Tsr H3.mpg). Moreover, four different point mutations introduced into this construct restored Tsr function, as assessed on semi-solid agar plates (Fig. 7A).

The location of all of the second-site suppressors in the protein-interaction region suggests that the partial attractant response displayed by Tsr H3 is due to some subtle alteration in the ability of this protein to switch to the off conformation. In free-swimming cells lacking the phosphatase CheZ, the presence of the V367I substitution had a dramatic effect in restoring the ability of Tsr H3 to respond to serine with an immediate smooth-swimming response (compare movies MDP1-TsrH3 and MDP1-TsrH3 V367I in *Supporting information*). Thus, this single-residue replacement allows a complete inhibition of CheA

activity upon attractant stimulation. V367 is strongly conserved in receptors of the 36H class, to which Tsr belongs. The equivalent position in receptors of the 34H class is mostly occupied by a strongly conserved isoleucine (Alexander and Zhulin, 2007). The V367I replacement has also been isolated previously in our lab as a functional suppressor of the non-functional protein CheW R62H (M. Cardozo, unpubl. results).

Of the other mutations that restore wild-type function to Tsr H3, one targets the highly conserved G390 residue at the hairpin turn. Two others are different replacements (S or H) at the trimer contact residue R409. All four substitutions affect Tsr function to some extent when introduced into the full-length receptor (Fig. S4). Although we are unable to draw strong conclusions about the mechanisms by which the suppressing mutations restore normal function to the Tsr H3 construct, it is evident that all of the residue changes are likely to alter packing of the helices in the protein-interaction domain.

Unlike Tsr H1 and Tsr H2, Tsr H3 had a normal baseline level of covalent modification, indicating that it was efficiently deamidated by CheB. However, it displayed only a modest increase in methylation in response to addition of serine (Fig. 4A), suggesting that the ligand-induced conformational change was insufficient to produce a strong methylation response. The fact that the Tsr H3* variants recovered a methylation response comparable to that of wild-type Tsr (Fig. 4B) reinforces the concept of a yin-yang inter-dependence of the signalling and methylation regions (Swain *et al.*, 2009).

Wild-type receptors with elevated modification levels have lower affinities for their specific attractants, which reduces their sensitivity to attractants (Bornhorst and Falke, 2000; Li and Weis, 2000; Sourjik and Berg, 2002). Tsr H3 becomes absolutely insensitive to serine in the absence of CheR and CheB (Fig. S1). We speculate that the partial lock-on character of this construct (evidenced by an increased ability to activate CheA and an only partial ability to inhibit kinase activity after stimulation with serine) turns into a full lock-on character in the absence of CheB-mediated deamidation, presumably because of a deficient transmission of the signal between the adaptation and the protein-interaction regions.

Mixed-class trimers of dimers and function

Tsr H3 was able to form trimers of dimers not only with itself, but also with full-length Tar (Fig. 5B), in spite of the different lengths of their cytoplasmic domains. However, Tsr H3 was strongly epistatic to Tar function in semi-solid minimal-aspartate agar plates (Fig. 2C), indicating that the mixed Tar-Tsr H3 trimers were defective for Tar signalling. The effect did not seem to be due to any of the functional defects of Tsr H3 *per se*, since all the serine-

sensing Tsr H3* receptors also strongly interfered with Tar function (Fig. 7B). We suggest that trimers composed of receptors with cytoplasmic domains of different lengths may contain distortions in the trimer itself, and/or in the cluster array, that disrupt normal receptor function. Notably, the expression of relatively high levels of Tar did not affect Tsr H3 V367I function in a significant way (Fig. S4), suggesting that the distortion in the mixed trimer mainly affects the signalling ability of the longer receptor.

This conclusion was reinforced by the analysis of the effect of expression of naturally occurring 34H-class receptors McpB or McpH from *R. sphaeroides* 2.4.1 in *E. coli* cells containing Tar as their only MCP. Both heterologous receptors clearly interfered with Tar function (Fig. 8B), and they were able to form mixed trimers of dimers as deduced from the results of competition assays (Fig. S2) and by direct cross-linking of cysteine-substituted McpB (Fig. 8C).

As schematically depicted in Fig. 9C, receptors belonging to the same length class can form functional trimers, composed of dimers of the same or different specificity (pure or mixed 36H-class trimers on the left, 34H-class trimer on the right). When receptors belonging to different classes form a mixed trimer, however, differences in length may cause distortions in the trimers and/or in the resulting cluster organization that affect the function of some of the component receptors (mixed 36H-34H trimer in the centre). This interpretation is consistent with an observation based on measurements of chemoreceptor cluster cryo-tomograms from different species, which suggest that natural chemoreceptor clusters are composed of MCPs of a single length class (Briegel *et al.*, 2009).

Final considerations

Our results support the view that similar lengths of the N- and C-helices that form the conserved coiled-coil four-helix bundle within the cytoplasmic domain are critical for chemoreceptor function. However, the question remains open whether all of the specific interactions between matching heptads in the N- and C-helices need to be preserved, or if some are less critical. It is likely that the interaction between matching heptads in the methylation region and protein-interaction regions is crucial and that any alteration in the symmetry of these regions would cause profound deleterious effects. However, within the presumably less-constrained flexible region, a deletion of, for example, the 14th heptad in the N-helix (the deletion we made in Tsr) might be functionally compensated by deletion of the 24th heptad in the C-helix, as well as by deletion of its normal partner, the 23rd heptad. Such a combination would also restore heptad symmetry within the flexible region. However, the indel pattern observed in

natural MCPs does not support this scenario but rather suggests a view in which multiple specific interactions between pairs of heptads in the N-helix and C-helix are required, thus limiting the indels to ones that preserve the nature of the conserved knob-and-socket junctions that seem to be so central to proper function. More experiments will be needed to address this issue.

Experimental procedures

Bacterial strains

Strains were derivatives of the *E. coli* K12 strain RP437 (Parkinson and Houts, 1982) and carried the following genetic markers relevant to this study: strains UU1250 [Δ*aer-1* Δ*tsr-7028* Δ*(tar-tap)5201* Δ*trg-100*] (Ames *et al.*, 2002); UU1535 [Δ*aer-1* Δ*(tar-cheB)2234* Δ*tsr-7028* Δ*trg-100* *ygjG*::Gm *zbd*::Tn*5*] (Bibikov *et al.*, 2004); UU1581 [(*flhD-flhB*)*4* Δ*(tsr)-7028* Δ*(trg)-100*] (Studdert and Parkinson, 2005); UU1613 [*tar-S364C* Δ*(tsr)7028* Δ*(trg)100* Δ*(tap-cheB)-2234* Δ*(cheA-cheW)2167* *zec*::Tn*10-980*] (Studdert and Parkinson, 2005); UU1624 [Δ*(tsr)7028* Δ*tap-3654* Δ*trg-100* Δ*aer-1*] (Gosink *et al.*, 2006); UU1626 [Δ*(cheA-tap)2260* Δ*(tsr)7028* Δ*(trg)100* Δ*(aer)1*] (Cardozo *et al.*, 2010); UU1935 [*mutD5* Δ*(flhD-flhA)4* Δ*(tsr)7028* Δ*(trg)100*] (P. Ames, unpublished); MDP1[tsr::Tn5 Δ*(cheZ)m-6725*] (this work); UU1615 [Δ*aer-1* Δ*(tar-tap)5201* Δ*trg-100*] (Gosink *et al.*, 2006); MDP14 [*tsr H3 V367I* Δ*aer-1* Δ*(tar-tap)5201* Δ*trg-100*] (this work).

Rhodobacter sphaeroides 2.4.1, used for amplification of the *mcpB* and *mcpH* genes, was a gift from Dr Georges Dreyfus (Departamento de Genética Molecular, Instituto de Fisiología Celular, Universidad Nacional Autónoma de México).

Plasmids

Parental plasmids derived from pACYC184 (Chang and Cohen, 1978), which confers chloramphenicol resistance and has sodium salicylate-inducible expression of the cloned gene, were pKG116 [salicylate-inducible expression vector] (Burón-Barral *et al.*, 2006), pCS12 [salicylate-inducible wild-type *tsr*] (Studdert and Parkinson, 2005), pDM113 [salicylate-inducible wild-type *tar*] (this work), pFG2 [salicylate-inducible wild-type *mcpB* from *R. sphaeroides* 2.4.1] (this work) and pK5 [salicylate-inducible wild-type *mcpH* from *R. sphaeroides* 2.4.1] (this work).

Plasmids encoding the heptad-deletion variants were obtained by site-directed mutagenesis, as described below, and were: pTsr H1 [salicylate-inducible *tsr* Δ(352–358)], pTsr H2 [salicylate-inducible *tsr* Δ(424–430)] and pTsr H3 [salicylate-inducible *tsr* Δ(352–358) Δ(424–430)].

The plasmid used in receptor-clustering assays was pPA803, a pRR48 derivative that confers ampicillin resistance and expresses a functional YFP–CheR fusion protein under inducible isopropyl β-D-thiogalactopyranoside (IPTG) control (Zhou *et al.*, 2011). pRR48 is a derivative of pBR322 (Bolivar *et al.*, 1977) that confers ampicillin resistance and has an expression/cloning site with a *tac* promoter and an ideal (perfectly palindromic) *lac* operator under the control of a plasmid-encoded LacI repressor (Studdert and Parkinson, 2005).

Site-directed mutagenesis

Cysteine reporters and heptad deletions were introduced with the QuikChange Site-Directed Mutagenesis Kit (Stratagene). For heptad deletions, pCS12 was used as the template plasmid. Candidate mutants were verified by sequencing the entire protein-coding region.

Immunoblotting

Cells were pelleted by centrifugation (6000 g) and resuspended at an OD_{600} of 2 in 10 mM potassium phosphate (pH 7.0) and 0.1 mM EDTA. Cells from 0.5 ml of the suspension were pelleted and lysed by boiling in 50 μl of sample buffer (Laemmli, 1970). Proteins released from the lysed cells were analysed by electrophoresis in SDS-PAGE and visualized by immunoblotting with an antiserum directed against the highly conserved portion of the Tsr signalling domain (Ames and Parkinson, 1994). A Cy5-labelled anti-rabbit immunoglobulin (Amersham) was used as secondary antibody. Fluorescence was detected with a Storm 1860 fluorimager (Amersham).

Chemotaxis assay in semi-solid agar plates

For Tsr function, cells carrying the pKG116 vector control or pCS12 derivatives were inoculated on tryptone semi-solid agar plates (1% tryptone, 0.5% NaCl, 0.25% agar) containing 12.5 μg ml⁻¹ chloramphenicol and 0.45 μM sodium salicylate. The plates were incubated for 7–10 h at 30°C.

For Tar function, UU1624 cells (carrying a chromosomal copy of the tar gene as the only MCP) transformed with the pKG116 vector control or pCS12 derivatives were inoculated into minimal H1 semi-solid agar plates (Hazelbauer *et al.*, 1989) containing chloramphenicol (12.5 μg ml⁻¹) and different concentrations of sodium salicylate, supplemented with 0.15 mM aspartate and 2 mM glycerol. The plates were incubated for 20 h at 30°C.

Tethered-cell assay

UU1250, UU1535 or MDP1 cells expressing wild-type Tsr or its derivatives were tethered to microscope slides with anti-flagellin antiserum, as described (Parkinson, 1976), and examined under a phase-contrast microscope, in the absence or presence of L-serine. For each strain, at least 100 rotating cells were observed for 15 s each and classified into one of five categories according to their sense of rotation. Cells were observed within 3 min after the addition of the attractant. The overall per cent of time spent in CW rotation was computed as a weighted sum: the per cent of cells that rotated exclusively CW, plus 0.75× the per cent of cells rotating predominantly CW, plus 0.5× the per cent of cells reversing frequently, plus 0.25× the per cent of cells rotating predominantly, but not exclusively, CCW.

Observation of free-swimming cells

Cells expressing the Tsr variants were grown to mid-log phase, harvested by centrifugation (1000 *g*), washed twice with 10 mM potassium phosphate (pH 7.0), 0.1 mM EDTA, and finally resuspended in the same buffer plus 10 mM lactate, 1 mM methionine and 200 µg ml⁻¹ chloramphenicol.

Swimming cells were observed under an inverted phase-contrast microscope (Nikon, Eclipse Ti) and recorded for several seconds before, and at several intervals after, the addition of L-serine (100 µM final concentration), using a Nikon Coolpix S10 camera.

Tsr methylation assay

UU1626 cells transformed with pCS12 derivatives were grown at 30°C to mid-log phase in tryptone broth with 0.45 µM sodium salicylate, harvested by centrifugation, washed three times with 10 mM potassium phosphate (pH 7.0), 0.1 mM EDTA, and finally resuspended at $OD_{600} = 1$ in the same buffer plus 10 mM lactate, 1 mM methionine and 200 µg ml⁻¹ chloramphenicol. After 15 min incubation at 30°C, cell suspensions (0.5 ml) were challengeded with 100 mM L-serine or with an equivalent volume of water for an additional 30 min. Cells were then pelleted and lysed by boiling in 50 µl of sample buffer. Proteins released from the lysed cells were analysed by SDS-PAGE in 11% acrylamide, 0.075% bisacrylamide gels and visualized by immunoblotting with Tsr antiserum.

TMEA cross-linking

Cells were grown at 30°C to mid-log phase in tryptone broth containing 25 µg ml⁻¹ of chloramphenicol and the appropriate concentrations of sodium salicylate, harvested by centrifugation, and resuspended at $OD_{600} = 2$ in 10 mM potassium phosphate (pH 7) and 0.1 mM EDTA. Cell suspensions (0.5 ml) were incubated for 10 min at 30°C and then treated with 50 µM TMEA (Pierce) for 20 s at 30°C. Reactions were quenched by the addition of 10 mM N-ethylmaleimide. Cells were pelleted and then lysed by boiling in 50 µl of sample buffer. Proteins released from the lysed cells were analysed by SDS-PAGE in 10% acrylamide, 0.05% bisacrylamide gels and visualized by immunoblotting with Tsr antiserum.

Receptor-clustering assay

Receptor clusters were visualized by fluorescence light microscopy in cells expressing a YFP–CheR fusion protein as a reporter. Cells containing pPA803 (YFP–CheR under IPTG control) and the vector control plasmid pKG116 or different pCS12 derivatives were grown at 30°C in tryptone broth to mid-log phase in the presence of 100 µM IPTG and 0.45 µM sodium salicylate. Cells were collected and examined essentially as described (Sourjik and Berg, 2000). Cell fields were photographed and at least 100 cells were inspected by eye to determine the proportion of individual cells with one or more distinct bright spots of fluorescence, which are indicative of a receptor cluster.

Isolation of second-site suppressor mutations

To identify second-site mutations that suppressed the chemotaxis defects exhibited by the Tsr H1–H3 variants, plasmids encoding those variants were mutagenized by passage through UU1935, a proofreading-deficient polymerase mutant (Cox and Horner, 1986). Plasmid preparations obtained from this strain (pTsr H1–H3* variants) were electroporated into UU1250 cells. Transformants were selected on tryptone semi-solid agar plates containing chloramphenicol (12.5 µg ml⁻¹) and salicylate (0.45 µM). After incubation at 30°C for 14–20 h, cells from outgrowing chemotaxis rings were picked, and colonies were purified on selective antibiotic medium. The pTsr H* plasmids were purified, used to re-transform UU1250 cells, and tested for suppressor properties in tryptone semi-solid agar plates, using the parental plasmid and wild-type Tsr-encoding pCS12 as negative and positive controls respectively.

References

Alexander, R.P., and Zhulin, I.B. (2007) Evolutionary genomics reveals conserved structural determinants of signaling and adaptation in microbial chemoreceptors. *Proc Natl Acad Sci USA* **104:** 2885–2890.

Ames, P., and Parkinson, J.S. (1994) Constitutively signaling fragments of Tsr, the *Escherichia coli* serine chemoreceptor. *J Bacteriol* **176:** 6340–6348.

Ames, P., Studdert, C.A., Reiser, R.H., and Parkinson, J.S. (2002) Collaborative signaling by mixed chemoreceptor teams in *Escherichia coli*. *Proc Natl Acad Sci USA* **99:** 7060–7065.

Bibikov, S.I., Miller, A.C., Gosink, K.K., and Parkinson, J.S. (2004) Methylation-independent aerotaxis mediated by the *Escherichia coli* Aer protein. *J Bacteriol* **186:** 3730–3737.

Bolivar, F., Rodriguez, R.L., Greene, P.J., Betlach, M.C., Heyneker, H.L., and Boyer, H.W. (1977) Construction and characterization of new cloning vehicles. II. A multipurpose cloning system. *Gene* **2:** 95–113.

Bornhorst, J.A., and Falke, J.J. (2000) Attractant regulation of the aspartate receptor-kinase complex: limited cooperative interactions between receptors and effects of the receptor modification state. *Biochemistry* **39:** 9486–9493.

Briegel, A., Ortega, D.R., Tocheva, E.I., Wuichet, K., Li, Z.,

Chen, S., *et al*. (2009) Universal architecture of bacterial chemoreceptor arrays. *Proc Natl Acad Sci USA* **106:** 17181–17186.

Burón-Barral, M.C., Gosink, K.K., and Parkinson, J.S. (2006) Loss- and gain-of-function mutations in the F1-HAMP region of the *Escherichia coli* aerotaxis transducer Aer. *J Bacteriol* **188:** 3477–3486.

Cardozo, M.J., Massazza, D.A., Parkinson, J.S., and Studdert, C.A. (2010) Disruption of chemoreceptor signalling arrays by high levels of CheW, the receptor-kinase coupling protein. *Mol Microbiol* **75:** 1171–1181.

Chang, A.C., and Cohen, S.N. (1978) Construction and characterization of amplifiable multicopy DNA cloning vehicles derived from the P15A cryptic miniplasmid. *J Bacteriol* **134:** 1141–1156.

Coleman, M.D., Bass, R.B., Mehan, R.S., and Falke, J.J. (2005) Conserved glycine residues in the cytoplasmic domain of the aspartate receptor play essential roles in kinase coupling and on-off switching. *Biochemistry* **44:** 7687–7695.

Cox, E.C., and Horner, D.L. (1986) DNA sequence and coding properties of mutD(dnaQ) a dominant *Escherichia coli* mutator gene. *J Mol Biol* **190:** 113–117.

Draheim, R.R., Bormans, A.F., Lai, R.Z., and Manson, M.D. (2005) Tryptophan residues flanking the second transmembrane helix (TM2) set the signaling state of the Tar chemoreceptor. *Biochemistry* **44:** 1268–1277.

Gestwicki, J.E., Lamanna, A.C., Harshey, R.M., McCarter, L.L., Kiessling, L.L., and Adler, J. (2000) Evolutionary conservation of methyl-accepting chemotaxis protein location in Bacteria and Archaea. *J Bacteriol* **182:** 6499–6502.

Gosink, K.K., Buron-Barral, M.C., and Parkinson, J.S. (2006) Signaling interactions between the aerotaxis transducer Aer and heterologous chemoreceptors in *Escherichia coli*. *J Bacteriol* **188:** 3487–3493.

Hazelbauer, G.L., and Lai, W.C. (2010) Bacterial chemoreceptors: providing enhanced features to two-component signaling. *Curr Opin Microbiol* **13:** 124–132.

Hazelbauer, G.L., Park, C., and Nowlin, D.M. (1989) Adaptational 'crosstalk' and the crucial role of methylation in chemotactic migration by *Escherichia coli*. *Proc Natl Acad Sci USA* **86:** 1448–1452.

Hazelbauer, G.L., Falke, J.J., and Parkinson, J.S. (2008) Bacterial chemoreceptors: high-performance signaling in networked arrays. *Trends Biochem Sci* **33:** 9–19.

Hulko, M., Berndt, F., Gruber, M., Linder, J.U., Truffault, V., Schultz, A., *et al*. (2006) The HAMP domain structure implies helix rotation in transmembrane signaling. *Cell* **126:** 929–940.

Kim, K.K., Yokota, H., and Kim, S.H. (1999) Four-helical-bundle structure of the cytoplasmic domain of a serine chemotaxis receptor. *Nature* **400:** 787–792.

Lacal, J., Garcia-Fontana, C., Munoz-Martinez, F., Ramos, J.L., and Krell, T. (2010) Sensing of environmental signals: classification of chemoreceptors according to the size of their ligand binding regions. *Environ Microbiol* **12:** 2873–2884.

Laemmli, U.K. (1970) Cleavage of structural proteins during the assembly of the head of bacteriophage T4. *Nature* **227:** 680–685.

Le Moual, H., and Koshland, D.E., Jr (1996) Molecular evolution of the C-terminal cytoplasmic domain of a superfamily of bacterial receptors involved in taxis. *J Mol Biol* **261:** 568–585.

Li, G., and Weis, R.M. (2000) Covalent modification regulates ligand binding to receptor complexes in the chemosensory system of *Escherichia coli*. *Cell* **100:** 357–365.

Maddock, J.R., and Shapiro, L. (1993) Polar location of the chemoreceptor complex in the *Escherichia coli* cell. *Science* **259:** 1717–1723.

Massazza, D.A., Parkinson, J.S., and Studdert, C.A. (2011) Cross-linking evidence for motional constraints within chemoreceptor trimers of dimers. *Biochemistry* **50:** 820–827.

Parkinson, J.S. (1976) *cheA, cheB*, and *cheC* genes of *Escherichia coli* and their role in chemotaxis. *J Bacteriol* **126:** 758–770.

Parkinson, J.S., and Houts, S.E. (1982) Isolation and behavior of *Escherichia coli* deletion mutants lacking chemotaxis functions. *J Bacteriol* **151:** 106–113.

Sourjik, V., and Berg, H.C. (2000) Localization of components of the chemotaxis machinery of *Escherichia coli* using fluorescent protein fusions. *Mol Microbiol* **37:** 740–751.

Sourjik, V., and Berg, H.C. (2002) Receptor sensitivity in bacterial chemotaxis. *Proc Natl Acad Sci USA* **99:** 123–127.

Starrett, D.J., and Falke, J.J. (2005) Adaptation mechanism of the aspartate receptor: electrostatics of the adaptation subdomain play a key role in modulating kinase activity. *Biochemistry* **44:** 1550–1560.

Studdert, C.A., and Parkinson, J.S. (2004) Crosslinking snapshots of bacterial chemoreceptor squads. *Proc Natl Acad Sci USA* **101:** 2117–2122.

Studdert, C.A., and Parkinson, J.S. (2005) Insights into the organization and dynamics of bacterial chemoreceptor clusters through *in vivo* crosslinking studies. *Proc Natl Acad Sci USA* **102:** 15623–15628.

Swain, K.E., Gonzalez, M.A., and Falke, J.J. (2009) Engineered socket study of signaling through a four-helix bundle: evidence for a yin-yang mechanism in the kinase control module of the aspartate receptor. *Biochemistry* **48:** 9266–9277.

Walshaw, J., and Woolfson, D.N. (2003) Extended knobs-into-holes packing in classical and complex coiled-coil assemblies. *J Struct Biol* **144:** 349–361.

Wuichet, K., and Zhulin, I.B. (2010) Origins and diversification of a complex signal transduction system in prokaryotes. *Sci Signal* **3:** ra50.

Xu, Q., Black, W.P., Nascimi, H.M., and Yang, Z. (2011) DifA, a methyl-accepting chemoreceptor protein-like sensory protein, uses a novel signaling mechanism to regulate exopolysaccharide production in *Myxococcus xhantus*. *J Bacteriol* **193:** 759–767.

Yeh, J.I., Biemann, H.P., Pandit, J., Koshland, D.E., and Kim, S.H. (1993) The three-dimensional structure of the ligand-binding domain of a wild-type bacterial chemotaxis receptor. Structural comparison to the cross-linked mutant forms and conformational changes upon ligand binding. *J Biol Chem* **268:** 9787–9792.

Zhang, P., Khursigara, C.M., Hartnell, L.M., and Subramaniam, S. (2007) Direct visualization of *Escherichia coli* chemotaxis receptor arrays using cryo-electron microscopy. *Proc Natl Acad Sci USA* **104:** 3777–3781.

Zhou, Q., Ames, P., and Parkinson, J.S. (2011) Biphasic control logic of HAMP domain signalling in the *Escherichia coli* serine chemoreceptor. *Mol Microbiol* **80:** 596–611.

Supporting information

Additional supporting information may be found in the online version of this article.

Please note: Wiley-Blackwell are not responsible for the content or functionality of any supporting materials supplied by the authors. Any queries (other than missing material) should be directed to the corresponding author for the article.